RSC Advances

ROYAL SOCIETY OF CHEMISTRY

www.rsc.org/advances

Journal Name

ARTICLE

Biological relevance of oxidative debris present in as-prepared graphene oxide

Received 00th January 20xx,
Accepted 00th January 20xx

DOI: 10.1039/x0xx00000x

www.rsc.org/

Ajith Pattammattel[a,b,c], Christina L. Williams[a,b], Paritosh Pande[a] William G. Tsui[a], Ashis K. Basu[a] and Challa Vijaya Kumar[a,b,c]*

The influence of oxidative debris (OD) present in as-prepared graphene oxide (GO) suspensions on proteins and its toxicity to human embryonic kidney cells (HEK-293T) are reported here. The OD was removed by repeated washing with aqueous ammonia to produce the corresponding base-washed GO (bwGO). The loading (w/w) of bovine serum albumin (BSA) was increased by 85% after base wash, whereas the loading of hemoglobin (Hb) and lysozyme (Lyz), respectively, was decreased by 160% and 100%. The secondary structures of 13 different proteins bound to bwGO were compared with the corresponding proteins bound to GO using the UV circular dichroism spectroscopy. There was a consistent loss of protein secondary structure with bwGO when compared with proteins bound to GO, but no correlation between either the isoelectric point or hydrophobicity of the protein and the extent of structure loss was observed. All enzymes bound to bwGO and GO indicated significant activities, and a strong correlation between the enzymatic activity and the extent of structure retention was noted, regardless of the presence or absence of OD. At low loadings (<100 µg/mL) both GO and bwGO showed excellent cell viability but substantial cytotoxicity (~40% cell death) was observed at high loadings (>100 µg/mL). In control studies, OD by itself did not alter the growth rate even after a 48-h incubation. Thus, the presence of OD in GO played a very important role in controlling the chemical and biological nature of the protein-GO interface and the presence of OD in GO improved its biological compatibility when compared to bwGO.

Introduction

The role of oxidative debris (OD) present in as-prepared graphene oxide (GO) in influencing its interactions with a small set of biological samples such as proteins and cells are examined here. Interactions of proteins with graphene oxide (GO) are a subject of great interest for their potential applications in biology.[1] A clear understanding of the behavior and the effect of GO on biomolecules is essential for building functional, catalytic, sensing, medical, and artificial bio-systems with GO. Interactions of proteins with certain (nano)materials are well-studied, which allows one to predict their affinity, structure, and stability.[2] However, GO is a highly heterogeneous surface with oxygenated functional groups such as hydroxyls, carboxyls and epoxides that are randomly distributed in a hydrophobic 2D carbon basal plane, along with peripheral carboxylate functions at the edges of the sheets (Scheme 1). The heterogeneity of GO surface makes it more challenging to predict the behavior of biomolecules at its surface.[3]

Structural denaturation of proteins at GO, because of unfavorable interactions between GO and the hydrophobic protein interior, adversely affects the protein function.[4] Thus, several surface passivation approaches were established to mask unfavorable hydrophobic interactions [5] to prevent protein denaturation. Modulation in enzyme properties such as, decrease or increase in enzymatic activity,[4,5,6] and complete inhibition[7] on binding of enzymes to GO was illustrated before. The conformation and protein structure as well as its orientation at the nanosurface play major roles in determining bound enzyme activities.[7]

Chemical functionalization,[8] reduction, and passivation with intermediary proteins[9, 10] or polymers,[11] can successfully passify GO surface and stabilize certain proteins and enzymes. Reports suggest that the extent of surface hydrophobicity plays a major role in retaining protein structure and thereby bound enzyme function.[5] Recent advances in structural studies of GO have identified the presence of small, highly oxidized polycyclic aromatic moieties called oxidative debris (OD) in GO suspensions.[12] In addition, decrease in conductivity,[13]

[a] Department of Chemistry
[b] Department of Molecular and Cell Biology
[c] The Institute of Material Science, University of Connecticut, 55 North Eagleville Road, Unit 3060, Storrs, CT 06269-3060

† Electronic Supplementary Information (ESI) available: contains characterization of GO and bwGO, data analysis and enzymatic activity assay plots. See DOI: 10.1039/x0xx00000x

increase in fluorescence,[16] increased electrochemical activity[14] and decreased interactions of GO with small molecules[15] are attributed to the presence of OD on its surface. Treating GO with aqueous base solutions separates this debris (Scheme1), and the resulting base-washed GO (bwGO) has several desirable and improved properties.[16] Thus, an interesting question arises as to how and to what extent OD disturbs biological properties of GO? To date, no such investigation has been carried out to investigate the role of OD in controlling the interactions of GO with biological molecules or cells. Biological applications of GO are being currently actively pursued for a variety of reasons.[1, 17] Therefore, it is critical to analyze the nature of bio-GO interface in the absence of OD. Moreover, the structure of bwGO is closer to graphene than to GO and, therefore, it is important to examine the influence OD present in GO on its interactions with proteins, enzymes and other biomolecules.

Here, we report the role of OD at GO interface in controlling the properties of a set of 13 different proteins. These have increasing isoelectric points (pH where the net charge on the protein is zero, pI), molecular weights, and increasing number of surface arginines (SI, Table S1). Our results suggest that OD plays a major role in controlling binding affinities, as well as bound enzyme structure/activities. Binding to GO and bwGO, structure retention and enzymatic activities were analyzed using multiple methods (Scheme 1). Furthermore, cytotoxicity of GO, bwGO as well as OD and differences in their toxicities are examined here. Our current study gives an insight into the fundamental understanding of bio-GO interactions at molecular level such as the role of surface functionalities and their nature in determining the affinity, secondary structure, and enzymatic activities. This information would be valuable for the rational control of protein behavior at particular nanosurfaces.

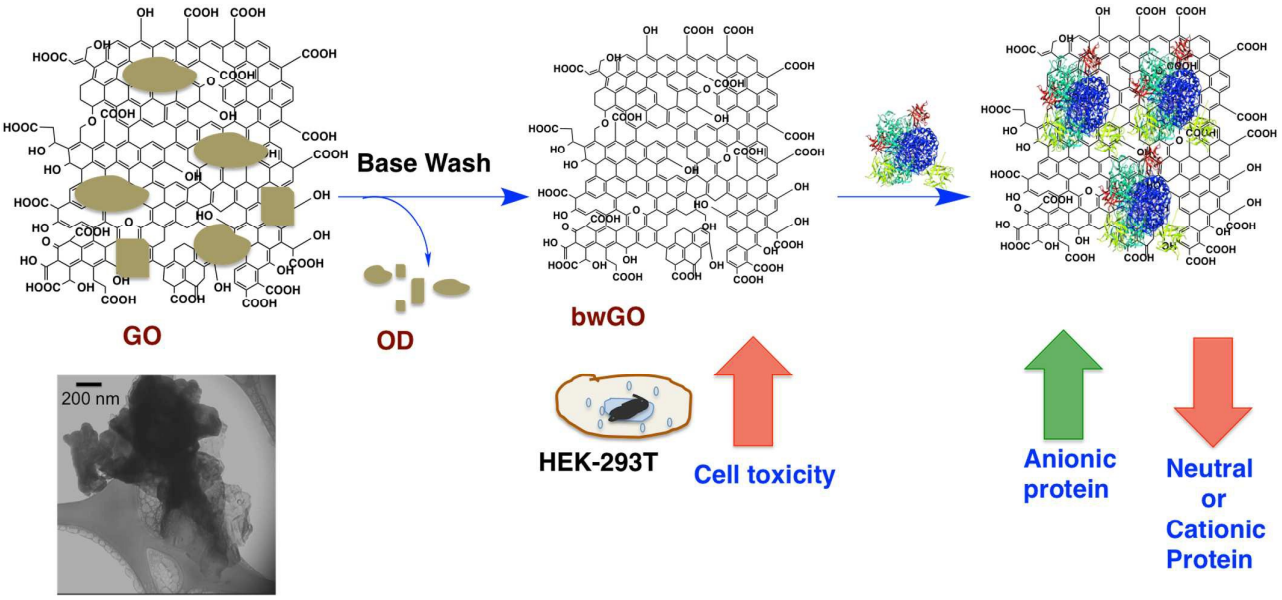

Scheme 1. Oxidative debris (OD) was removed from graphene oxide (GO), by washing with aqueous ammonia, and the influence of OD on enzyme-GO interface has been examined. OD protects the bound enzymes from structure/activity loss and decreases cytotoxicity.

Experimental

Materials

Graphite flakes, guaiacol, KMnO4, Glucose oxidase (GOx, Aspergillus niger), lysozyme (egg white), human serum albumin (HSA), RNase A, beta lactoglobulin (BLG), ovalbumin (egg white) and myoglobin (bovine) were purchased from Sigma Aldrich (St. Louis, MO). Horseradish peroxidase (HRP) and cytochrome *C* (equine heart) were obtained from Calzyme laboratories Inc. (San Luis Obispo, CA). Pepsin A, catalase and trypsin (Bovine) were bought from Worthington Biomedical Corporation (Lakewood, NJ). Met-hemoglobin (Hb, bovine) was purchased from MP Biomedicals, LLC (Solon, OH). The human embryonic kidney (HEK 293T) cells were purchased from American Type Culture Collection (ATCC, Manassas, VA) and the growth media components (Dulbecco's Modified Eagle Media (DMEM) and Fetal bovine serum (FBS)) were purchased from Gibco®. The metabolic activities of HEK 293T cells were analyzed with the Cell Counting Kit (CCK-8™) purchased from Dojindo Molecular Technologies Inc.

Methods

Preparation of GO and bwGO. GO was prepared by modified Hummers' Method as reported elsewhere.[18] bwGO was prepared by washing GO suspension with aqueous ammonia.[16] Base washing of GO with aqueous ammonia, when compared to NaOH, has practical advantages in obtaining pure OD without any solid NaCl (product of neutralization of NaOH with HCl at the end). Briefly, GO solution (2 mg/mL, 100 mL) was stirred with 40 mL aq. NH_3 at 100°C until the solution was separated into two different phases (~3 h). bwGO was separated from OD by repeated centrifugation, washed repeatedly with water (3-5 times) and re-suspended in 10 mM sodium phosphate buffer (pH 7.0). OD was obtained from the aqueous ammonia layer, after solvent evaporation.

Fluorescence quenching experiments. FlexStation® (Molecular Devices, Sunnyvale, CA) was used in a standard opaque 96 well plate with 0.250 mL volume for each well. BSA was labeled with fluorescein isothiocyanate (FITC), with the assumption that the quenching efficiency of bwGO and GO is nearly identical. BSA-FITC (1 μM) was titrated against different concentrations of GO (0.8 mg/mL) or bwGO (0.8 mg/mL). BSA-FITC emission and FITC emission at 525 nm (485 nm excitation) was used to tabulate the quenching data. The data were fit into modified Stern-Volmer equation, as reported before (equation 1),[10]

$$\frac{F_0}{F_0 - F} = \frac{1}{\left[(f_a K_a Q) + \frac{1}{f_a}\right]} \qquad \text{(Equation 1)}$$

where [Q] = quencher concentration; F_0 = Fluorescence intensity when [Q] = 0; F = Fluorescence intensity at given [Q]; K_a = Bimolecular quenching constant, and f_a = fraction of the initial fluorescence accessible to the quencher.

Protein binding studies. Stock solutions of proteins were prepared in 10 mM phosphate buffer pH 7.0. To determine the concentration, absorbance was measured (406 nm for Hb or 280 nm for lysozyme and other proteins). For Hb, a set of solutions with a concentration range of 5, 10, 15, 20, 25, and 30 μM were prepared in phosphate buffer pH 7.0 with 0.2 mg/mL GO and 0.2 mg/mL bwGO. For lysozyme, six solutions of concentrations 10, 20, 30, 40, 50, and 60 μM were prepared, equilibrated with same GO and bwGO concentrations (0.2 mg/mL). All suspensions were allowed to equilibrate for an hour and centrifuged for 20 min at 12,000 rpm to aspirate unbound proteins. Absorbance measurements were taken for the supernatant at the same wavelengths previously used to determine the protein concentrations. The adsorption isotherms were analyzed using Langmuir adsorption model, using equation 2,[19] to obtain the binding affinity and theoretical adsorption maxima.

$$Q = {KC_eQ_{sat}}\Big/{[1 + KC_e]} \text{------ (Equation 2)}$$

where, K is the dissociation constant (in μM), Q is the binding density at equilibrium (in μmol/mg), C_e is the protein concentration (in μM) and Q_{sat} is the saturation binding point.

Circular Dichroism Studies. Far UV CD spectra (260 – 190 nm) of protein solutions were recorded on a Jasco J-710 CD spectrometer (Easton, MD) before and after binding to GO or bwGO (0.20 mg/mL) using a 0.05 cm path length quartz cuvette. Protein to GO or bwGO ratio was kept same in all the samples as 50% (w/w) for fair comparison between proteins. All the spectra presented here were corrected for background signal from the buffer and normalized to 1 μM concentration of the protein. Any contributions to the CD signal due to the suspensions has been corrected and very short path length cells (0.05 cm) were used to minimize the correction. Relative structure retention of the conjugates was compared using ellipticity at 222 nm of the unbound protein as a standard.

Activity Studies. Solutions of hemoglobin (Hb, 8 μM), myoglobin, (Mb, 12 μM), catalase (Cat, 0.8 μM) and glucose oxidase (GOx, 4 μM) equilibrated with GO or bwGO (0.2 mg/mL) in pH 7.0 phosphate buffer at 25 °C. Peroxidase-like activities[20] of Hb and Mb were performed and compared with those bound to GO or bwGO. For the activity assay, 1 to 1.5 μM Hb or Mb, 2.5 mM guaiacol, and 4 mM H_2O_2 were reacted in pH 7.0 phosphate buffer and the activity was monitored by following the absorbance of the oxidation product at 470 nm. For catalase activity, 0.1 μM catalase and 20 mM H_2O_2 were reacted in pH 7.0 phosphate buffer and decomposition of H_2O_2 monitored at 240 nm.[21] GOx activity was assayed using horseradish peroxidase by known protocol.[22]

Cytotoxicity assay. The cytocompatibilities of OD, GO, and bwGO were investigated by co-incubation with human embryonic kidney cells (HEK 293T), one of the well-characterized and widely used human cell lines available. The standard growth conditions of 37 °C, 5% CO_2 and 95% relative humidity (RH) were maintained throughout the experiment and the intracellular metabolic rate determined using CCK-8 kit as reported.[23, 24]

Briefly, 0.5 x 10^5 cells were seeded in each well of a 24 well plate in 500 μl of complete growth media [Dulbecco's Modified Eagle media (DMEM) supplemented with 10% fetal bovine serum (FBS)] and incubated for 24 h to achieve a metabolically active early-log phase (1.0 X 10^5 cells). The GO, bwGO and OD samples were dispersed in phosphate buffered saline (PBS, 10 mM, pH 7.0) and sonicated for 1 h as reported earlier.[25]

The suspensions were further diluted with cell culture media and quickly vortexed before they were introduced to the adherent cells at a concentration range of 10, 25, 50, 75, 100, 250 and 500 µg/mL. During the co-incubation phase, the cell morphology was constantly monitored using light microscopy. The intracellular metabolic rate was assessed after 24 h of co-incubation by using CCK-8 kit that contains a tetrazolium salt, WST-8, which got reduced by dehydrogenase activity of live cells to generate a yellow-colored formazan dye. The amount of formazan dye generated, was quantified spectrophotometrically at 450 nm and it is directly proportional to the number of living cells. Appropriate negative controls, where the CCK-8 kit reagent (50 µl per well) was substituted with equal volume of PBS, were used for each concentration of GO, bwGO and OD whereas the positive control consisted of 50 µl of WST-8 solution added to the pristine cells grown in 500 µL of growth media. The data were analysed by standard statistical methods.

Results

The presence of OD has been shown to have a role in determining the chemical and biological properties of GO. The interactions of OD-free GO and bwGO with proteins are significantly different from that of GO, which influenced their structural and functional properties. The cell toxicity levels of bwGO and OD are compared with that of GO, and an increase in toxicity is noted after the removal of OD. Detailed descriptions of our results follow.

Preparation and characterization of bwGO. The as-prepared GO[18] was subjected to repeated washing with aqueous ammonia, washed with deionized water to remove the base, and we characterized the resulting bwGO as well as the oxidative debris by fluorescence spectroscopy (SI, Figure S1 A and B), and Raman spectroscopy (SI, Figure S2A). The quantity of OD accounted for ~30% (w/w) in a 100 mL, 1 mg/mL GO suspension. While the bwGO and GO showed no fluorescence upon excitation at 350 nm, OD indicated broad emission centered around 440 nm,[16] which is consistent with the presence of polycyclic aromatic debris in OD. The Raman spectra of GO and bwGO are essentially the same with D band at 1350 cm-1 and G band centered around 1600 cm^{-1} (SI Figure S2.A), as reported in the literature.[14] These identical Raman signals before and after base-wash indicated that there have been no additional defect sites introduced in bwGO upon the base wash. No significant change in I_D/I_G ratio of bwGO compared to GO confirms that no reduction of GO occurred during the washing process. The morphology of GO and bwGO is compared using their respective TEM images (Figure S2.B), which shows that the layered structure is preserved after base wash. Next, these samples were tested for their interactions with proteins, as model biological systems of interest.

Protein binding studies. We examined the interactions of a few proteins such as bovine serum albumin (BSA, pI 4.2), met-hemoglobin (Hb, 7.0), lysozyme (Lyz, pI=12) and ten other proteins (SI, Table S1) in binding studies with GO and bwGO. We labeled BSA with fluorescein-isothiocyanate (FITC) and examined its binding to GO in quenching studies. GO quenches BSA-FITC fluorescence and binding has been monitored as a function of increasing concentrations of GO, at fixed BSA-FITC concentration.[10] The quenching data have been analyzed by reported methods (Figure 1) to estimate the binding affinities (K_a).

Figure 1. Quenching of fluorescence of FITC labeled BSA (BSA-FITC) by the addition of

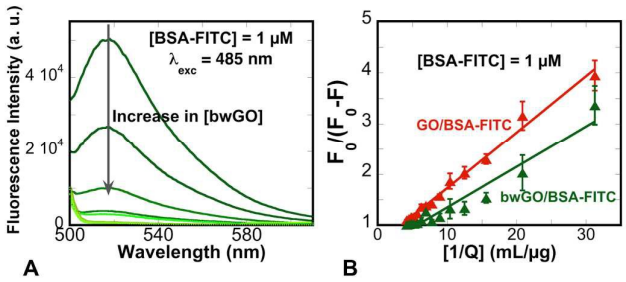

GO or bwGO due to binding to the nanosheets A. Fluorescence spectra of BSA-FITC in the presence of increasing concentrations of bwGO upon excitation at 485 nm. B. Stern-Volmer fit for the quenching of BSA-FITC emission by GO (red line) or bwGO (green line). The corresponding affinity constants are 5.7 (±0.8) x 10^3 mL/mg and 6.8 (±1.2) x 10^3 mL/mg for GO and bwGO, respectively.

Equation 1 was used to fit the quenching data where [Q] = quencher concentration (GO/bwGO); F_0 = Fluorescence intensity in the absence of quencher; F = Fluorescence intensity at given [Q]; K_a = Bimolecular affinity constant, and f_a = fraction of the initial fluorescence. Thus, from the slope ($1/K_af_a$) and y-intercept ($1/f_a$) of the fitted line, K_a was calculated.

The quenching constants were compared with the assumption that both bwGO and GO quench the fluorescence to the same extent, and K_a for GO 5.7 (±0.8) x 10^3 mL/mg and 6.8 (±1.2) x 10^3 mL/mg. Clearly, the affinity of BSA increased when OD has been removed.

The binding of proteins to GO and bwGO was also investigated in equilibrium binding studies, where the samples were equilibrated with protein solutions, and unbound protein has been separated by centrifugation. Unbound protein concentration was determined by its absorbance at 280 nm for BSA and lysozyme, while absorbance at 406 nm has been monitored for Hb samples. The corresponding adsorption isotherms are shown in Figure 2.

The affinity of BSA increased after the base wash (Figure 2A, green), which is in good agreement with the above fluorescence studies. In the cases of both Hb and Lyz,

the binding to bwGO was similar to that of GO (Figure 2B and 2C, red lines for GO and green lines for bwGO) at low protein concentrations of 5-10 μM for Hb and 10-20 μM for Lyz. But at higher concentrations (>10 and >20 for Hb and Lyz, respectively), protein loading on bwGO was less than that of GO, under the same conditions. Maximum loading (w/w) of BSA was increased after base-wash by 85%, that of Hb decreased by 160% and that of Lyz decreased by 100%. The binding of GOx to GO was negligible at low protein concentrations, while bwGO showed a maximal loading of 64% (SI Figure S3), and in case of GO it decreased to 52%.

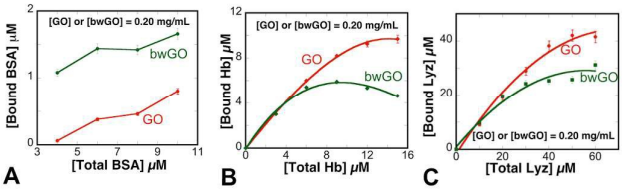

Figure 2. Binding isotherms of (A) BSA, (B) Hb and (C) Lyz with GO (0.20 mg/ml, red) and bwGO (0.20 mg/ml, green) in phosphate buffer, pH 7.0. Affinities increased from BSA to Hb to Lyz, which corresponded with increases in protein charge.

Langmuir model of Hb and Lyz adsorption to the nanosheets showed clear differences in binding affinities after base wash (Table 1). The K_a for Hb to GO was 1.9 (± 0.6) x 10^7 M^{-1}, whereas the affinity decreased substantially for bwGO (3.6 (± 2.1) x 10^6 M^{-1}). Lyz showed strong adsorption to GO with Ka of 8.1 (± 3.5) x 10^7 M^{-1}, and it decreased to 2.8 (± 0.8) x 10^7 M-1 for bwGO. The decrease in affinity is also reflected in the adsorption parameter, Q_{sat}, which represents theoretical maximum for monolayer formation of the protein (in μmol) per solid (in mg). As expected, Hb and Lyz showed significant drop in maximal loadings (2-3 fold), which suggests weaker adsorption of proteins to bwGO.

Table1. Parameters obtained by the analysis of the binding isotherms using the Langmuir adsorption isotherm (equation 2)[19]

System	K_a (M^{-1})	Maximal Loading, Q_{sat} (μmol/mg)	R^2
Hb /GO	1.9 (± 0.6) x 10^7	124 (± 26)	0.99
Hb/bwGO	3.6 (± 2.1) x 10^6	38 (± 8)	0.94
Lyz/GO	8.1 (± 3.5) x 10^7	530 (± 152)	0.98
Lyz/bwGO	2.8 (± 0.8) x 10^7	219 (± 26)	0.97

Zeta Potential Titrations. To further characterize the changes in bio-nano interactions, the zeta potential titrations of proteins with GO and bwGO were carried out (Figure 3). The Zeta potential of bwGO decreased from -33 mV (no protein added) to -18 mV when Hb concentration was increased from 0 to 22 μM, while that of GO increased from -35 to -12 mV over the same protein concentration range. This showed reduced binding affinity of Hb to bwGO, supporting the above adsorption studies. In contrast to Hb, Lyz showed essentially the same charge dependence either with GO or bwGO, when concentration increased from 0 to 20 μM.

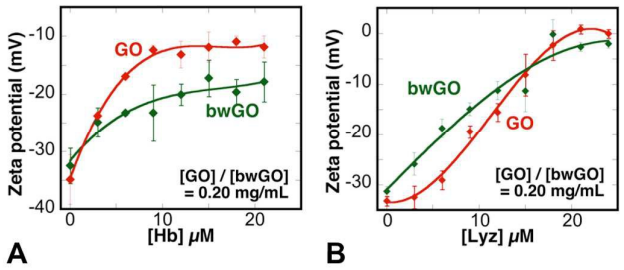

Figure 3. Zeta potential titrations of Hb (A), and Lyz (B) showed gradual charge neutralization during protein adsorption to GO (red) and bwGO (green).

Protein structure retention and circular dichroism studies. Nano-bio interactions influence bound protein structure, where strong interactions might distort or denature the protein. The extent of secondary structure retention was analyzed by examining the far–UV circular dichroism (CD) spectra of the bound protein. The extent of structure retention is approximated as the ratio of the ellipticity of the bound protein (E_{bound}) to that of the unbound protein ($E_{unbound}$), both measured at 222 nm, where the 222 nm minimum corresponds to the alpha helical content of the protein, which is estimated as RE@222 = (E_{bound} / $E_{unbound}$). Protein loading was kept at 50% (w/w), where all proteins showed significant binding to the nano sheets and spectra have been recorded using very short path length cuvettes (0.05 cm). The CD spectra were corrected for any scattering due to the suspensions, as reported earlier.[10,26]

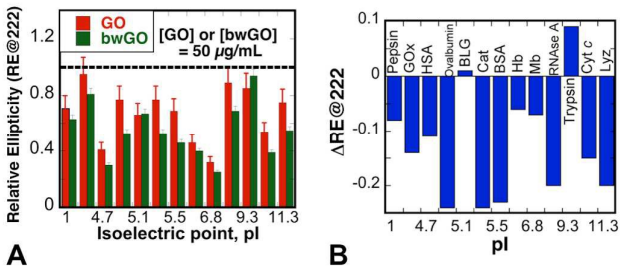

Figure 4. A. Plot of the ratios of ellipticities (RE@222) of bound proteins at 222 nm to that of the corresponding unbound protein as a function of protein pI values. Red bars correspond to those bound to GO and green bars correspond to those bound to bwGO. The ratio of 1.0 was taken for that of the unbound protein. B. Plot of ΔRE@222 as function of pI, where ΔRE@222= (RE@222 of protein bound to bwGO – RE@222 of the same protein bound to GO).

The ratio of ellipticities at 222 nm of GO-bound protein to that of the unbound protein (RE@222) indicated the order

GOx (pI - 4.6) > RNase (9.3) ≥ Trypsin (9.3) ≥ Ovalbumin (4.9) = Catalase (5.4) > Lyz (11.3) > Pepsin A (1.0) ≥ BSA (5.5) ≥ BLG (5.1) > Cyt *c* (10) > Hb (6.8) > HAS (4.7) > Mb (6.8) (Figure 4). In the case of bwGO, the trend was Trypsin > GOx > RNase ≥ BLG ≥ Pepsin A > Lyz ≥ Ovalbumin = Catalase > BSA > Hb ≥ Cyt *c* > HSA > Mb, but in almost all cases, the extent of structure retention was lower with bwGO than with GO.

A plot of the relative loss of structure when the protein is bound to GO vs bwGO was generated (Figure 4B) where the relative loss (ΔRE@222) is defined as RE@222 of a protein bound to bwGO minus the RE@222 of the same protein bound to GO. A positive value of this parameter indicates gain in protein secondary structure while a negative value corresponds to further loss in structure due to base-wash. The data show that maximal loss in structure occurred when the pI of the protein is close to neutral value, or when the protein has ~ -15 charge. This consistent loss in secondary structure could result in decreased enzymatic activities for the bound enzymes, and hence activities of enzymes bound to bwGO were determined and compared with those bound to GO.

Enzymatic activities. The peroxidase like activity of Hb and Mb, oxidase activity of GOx and reductase activity of Cat were assayed before and after binding to GO as well as bwGO, and the data have been compared to deduce the influence of base-wash on the bound enzyme activities. The per cent activities of samples bound to GO or bwGO with respect to those of the corresponding unbound proteins (100%) are shown in Figure 5.

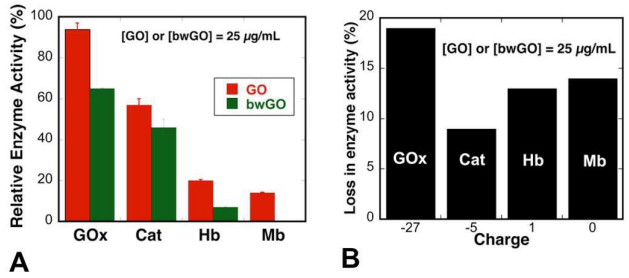

Figure 5. (A) Relative enzymatic activities of GO/enzyme (red bars), and bwGO/enzyme (green bars). B. Plot of activity loss enzymes bound to bwGO vs enzyme charge, which shows lack of correlation between activity loss and enzyme charge.

Oxidase activity of GO/GOx was essentially the same (94%) as that of the pristine GOx, but significant reduction has been noted (65%) in case of bwGO/GOx. Peroxidase-like activity of Hb was only 20% upon binding to GO and it reduced further to 5% on binding to bwGO. Similarly, GO/Mb showed only 14% activity and no measurable activity has been noted for bwGO/Mb. In case of Cat, the activity was reduced to ~60% on binding to GO while the activity of bwGO/Cat has been decreased to 45%.

A plot of loss in activity vs enzyme charge (Figure 5B) indicated a poor correlation with charge, which suggests that electrostatic interactions do not control the enzyme activity at this interface. To further test these conclusions, we have examined the influence of these materials on cell growth or cell viability using HEK 293T cells.

Cell toxicity studies. The cytocompatibility of GO, bwGO and OD with HEK 293T cells up to 24 h of co-incubation was evaluated, the data was obtained by (i) measuring intracellular metabolism indicated by spectrophotometric measurement of dehydrogenase activity within the cell and (ii) by observing the extracellular morphology using light microscopy and they showed no appreciable change in cell metabolism with respect to controls. After co-incubation for 24 h, the cells revealed a clear dose-dependent decrease in cell metabolism beyond 75 μg/mL (Figure 6). At higher loadings, bwGO was slightly more toxic than GO, within our experimental errors but both solids were toxic to the cells.

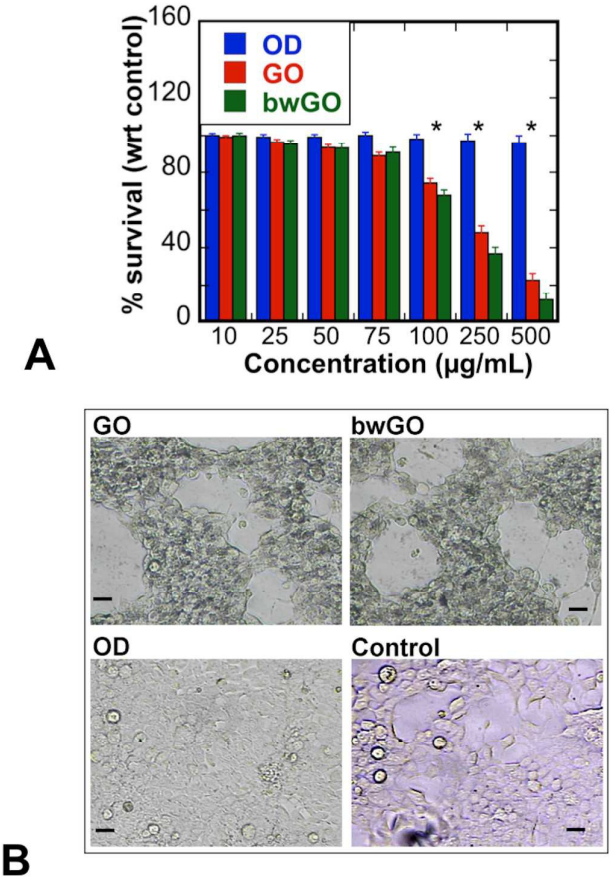

Figure 6. Cytotoxicity assays of GO, bwGO and OD when co-incubated with HEK 293T cells for 24 h. (A) Survival of the cells in comparison to the control shows that the dose-dependent toxicity of bwGO is higher than that of GO, and OD has no toxic effect. (B) Optical microscopy images of HEK 293T cells co-incubated with 500 μg/mL of GO (top, left), bwGO top, right), OD bottom, left) and Control HEK 293 T (bottom, right) for 36 h. Clearly, the cell morphology is affected by the presence of GO and bwGO (500 μg/mL), whereas OD did not affect cell growth. The difference in cell toxicity induced by GO and

bwGO was calculated using two-tailed unpaired student's *t* test, and it found to be statistically significant at concentrations above 75 µg/mL (*$p < 0.05$).

The above intracellular metabolism results were substantiated by light microscopy images taken at 24 h and 36 h of co-incubation, which revealed significantly stressed cell morphology at the GO and bwGO concentrations beyond 75 µg/mL. Interestingly, at greater than 75 µg/mL, bwGO turned out to be slightly more cytotoxic than GO.

We also examined the cells exposed to OD isolated from washing GO, but no morphological or metabolic differences could be observed between cells incubated with OD and control HEK 293T cells. The results obtained from CCK-8 kit, for monitoring intracellular dehydrogenase activity and light microscopy for assessing the cell morphology correlated consistently throughout the trials.

To further investigate the influence of OD on these cells, they were detached and transferred to a six-well plate and monitored for an additional 48 h (this is beyond the first 36 h of co-incubation). By this time cells exposed to the higher doses of GO and bwGO started to die, whereas the control cells and cells exposed to OD were still metabolically active. No appreciable difference in the rate of cell division, morphology or cellular metabolism was observed between OD co-incubated and control cells.

In summary, the binding affinities of several proteins have decreased, and their structure retention and enzymatic activities (when relevant) have also been decreased when the OD has been removed from the GO suspensions. Thus, OD appears to play an important role in shielding these bio-macromolecules from any adverse interactions of the underlying graphitic surface. When the surface is coated with low loadings of BSA (400% (w/w)), the activities of both Hb and Mb have recovered and even exceeded those adsorbed onto GO. Cytotoxicity studies show that these materials are toxic to HEK 293T cells at high concentrations (>75 µg/ml) and long exposure times (>24 h).

Discussion

Biohybrid materials that are made of biomolecules and carbon based nanomaterials (such as carbon nanotubes and GO) are thought to offer superior (or improved) biocompatibility, sustainability and biodegradability over inorganic (nano)materials.[17, 27] GO, a water dispersible graphene derivative, is one of the promising candidates for rapidly growing biomaterials research.[1] Recently, the presence of oxidative debris within GO suspensions was detected,[12] which showed significant influence on the material properties of GO.[16, 15, 28, 29] However, the effect of OD on protein-GO interactions has not been evaluated yet. Here, we have studied the effect of OD in controlling the bound protein characteristics as well as the role of OD in its cytotoxicity to HEK 293T cell lines.

Adsorption of proteins to both GO and bwGO are marginally different when evaluated against a small set of 13 proteins whose pI values ranged from 4 to 12. The maximum loading observed for Hb (pI 6.8) with GO was 320% (w/w), and this translates into an average of ~ 1.3 layers of Hb on the nanosheets, if we assume that the protein occupies the entire surface (7.05×10^{-22} Å^2/g) and that the diameter the protein is unchanged upon binding to the nanosheets. Along these lines, Hb binding to bwGO saturated around an average of 0.7 layers, much less than that observed with GO. This decrease in the coverage could be due to at least two possible factors, 1) decrease in intrinsic affinity of Hb to bwGO, or 2) loss in the secondary structure of bound Hb such that it occupies a larger area on the nanosheets. In support of the former, the Hb binding affinity of Hb decreased 10-fold, from GO to bwGO. On the other hand, the CD data analysis indicated only 10% loss in the CD band intensities for Hb bound to bwGO when compared to that bound to GO. Therefore, the decrease in the maximum loading of Hb is more likely due to reduced affinity.

Similar analysis of the CD data of Lyz (ΔRE@222 = -18%), GOx (ΔRE@222 = -14%) and BSA (ΔRE@222 = -23%) also indicates that protein denaturation is not directly controlling the loading maxima. Therefore, the changes in interactions at bwGO vs GO could be responsible for the differences in affinities.

The function of biohybrids can be quite sensitive to the conformation of the bound protein.[30, 31] Current studies involving 13 different proteins revealed that there has been a small but consistent increased loss in protein structure with bwGO when compared to the proteins bound to GO. To further understand the basis for increased protein structure loss on bwGO, we examined if there is any correlation between structure loss and protein charge or the hydropathy index of the protein. The average hydropathy index[32] was calculated using Expasy Protparam tool and it indicated the order Cyt *c* > RNase A > Catalase > BSA = Lyz > HSA = Mb > GOx > BLG > Trypsin > Ovalbumin > Hb > Pepsin A, but this trend has no correlation with the observed trends in RE@222 or ΔRE@222 of these proteins bound to bwGO. The relative loss of ellipticity at 222 nm (ΔRE@222), which is a measure of the per cent structure retention when compared to that of the unbound protein, did not correlate with net charge on the protein (SI, Figure S6), or the lysine content of the protein (SI, Figure S7) or the sum of the number of lysine and arginine residues present in the protein (SI, Figure S8).

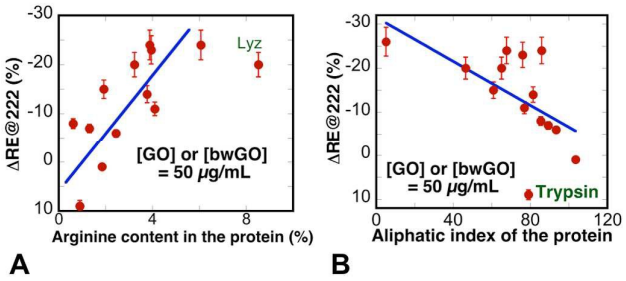

Figure 7. A. Correlation of the differential loss of ellipticities of GO and bwGO (ΔRE@222) with the protein arginine content. B. Plot of ΔRE@222 vs average volume occupied by aliphatic side chains of the protein, which was calculated using Expasy Protparam using the structures from the PDB.

On the other hand, the differences in the extents of structure loss when proteins bind to bwGO vs GO (ΔRE@222), however, depended on the percentage arginine content of the protein as well as the aliphatic index of the protein (Figure 7B). Twelve proteins containing Arg contents of 0-7% showed strong correlation with the extent of structure loss (Figure 7A), irrespective of their net charge. This strong trend shows the critical role of Arg residues in the interactions with bwGO. Arg was suggested to interact strongly with GO because of its ability to form hydrogen bonds as well as its charge and hydration status.[33,34,35] Lyz with 8% Arg content deviated significantly from the plot and could be due to its unusually high thermodynamic stability.[36] In a recent study, strong interaction of lysozyme, an arg rich protein, with carbon nanotubes (CNT) was demonstrated,[37] and the binding free energy (ΔG_{bind}) between strongly interacting Args in Lyz with CNT was -5.9 kcal/mol, higher than that of lysine (-3.5 kcal/mol).[38]

Interaction of the nanosurface with the amino acid side chains after base wash would influence bound protein conformation.[5] The possible role of hydrophobic residues in distorting the structure of the bound protein (between bwGO and GO) is examined in Figure 7B. The plot of extent of relative structure loss (ΔRE@222) as a function of the average aliphatic index showed a strong correlation. Aliphatic index is the volume occupied by the side chains of aliphatic amino acids (alanine, valine, isoleucine, and leucine) of the protein. There has been a greater retention of protein secondary structure with increasing aliphatic index. Base washing had less and less influence as the aliphatic index increased. That is, more hydrophobic proteins did not distinguish between bwGO and GO while less hydrophobic proteins are more sensitive to exposure to the hydrophobic surfaces of bwGO. Thus, the role of OD in these interactions depends also on the aliphatic index of the protein. Therefore, these afore mentioned correlations show that the interaction of bwGO with biomolecules is primarily via charged arginine as well as hydrophobic side chains, along with other specific interactions with surface functional groups of the nanosolid.

Correlation of the enzymatic activities of the enzymes bound to GO and bwGO was another tool used to compare the effect of OD. In support of our secondary structure studies, most showed decreases in activities when bound to bwGO vs GO, Figure 5A. Peroxidase like activity of Hb and Mb, reductase activity of Cat and, oxidase activity of GOx decreased at both interfaces and there has been no correlation with enzyme charge. Thus, hydrophobic interactions discussed above could be responsible for the structure loss which could result in activity loss. This possibility was examined next.

Further insight into the protein-GO interactions, thus, was evident when relative activities of the bound proteins are compared with their corresponding extents of secondary structure retention. A good linear correlation between enzyme secondary structure and enzymatic activity has been noted for Hb, Mb, Cat and GOx (Figure 8). Evidently, structural denaturation is the primary reason for the decrease in activity of the bound enzymes as the debris has been removed. This might seem trivial as structure retention is essential for activities but it has been noted that GO inhibited the activity of chymotrypsin[39] whereas GO has increased the activities of oxalate oxidase, esterase[5] and cytochrome *c*.[10]

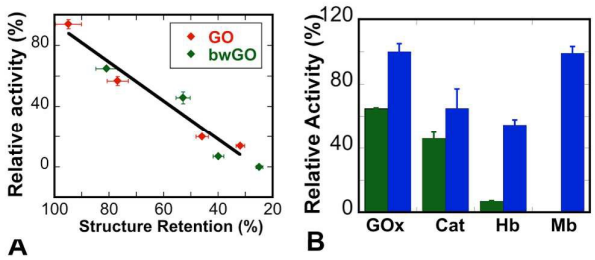

Figure 8. A. Strong correlation of relative activities of GOx, Cat, Hb and Mb bound to GO or to bwGO with the extents of their corresponding secondary structure retention. B. Blue bars correspond to bwGO samples that were biophilized with cationized BSA (BSA-bwGO/enzyme) before enzyme loading.

Since loss in activity is highly undesirable, we tested if the hydrophobic surfaces of bwGO could be passified by the adsorption of cationized BSA onto the nanosolid prior to enzyme loading.[10] BSA was chemically modified with the polyamine, tetraethelenepentamine (TEPA), which resulted in BSA charge reversal from -20 to +23 as confirmed by agarose gel electrophoresis. The bwGO surface (0.2mg/mL) was first passivated with cationized BSA (400% w/w), and Hb (8 μM), Mb (12 μM), Cat (0.8 μM) or GOx (4μM) were loaded onto the nanosolid. Activities of the above enzymes bound to cationized BSA-loaded bwGO (BSA-bwGO) are compared with those bound to bwGO, under similar conditions (Figure 8B). Surprisingly, the activities of GOx, Hb and Mb bound to BSA-bwGO exhibited substantial improvements (Figure 8B, blue bars) while Cat showed minor improvements.

Thus, the novel biofunctionalization strategy with cationized BSA to modify high energy nanosolids[10] can be successfully applied to passify bwGO for favourable enzyme loading.

Finally, the cell survival studies show that OD affects the interaction of GO with 293T cells. Incubation for 24 h, both GO and bwGO showed appreciable cytotoxicity above 75 µg/mL concentration (Figure 6). The dose dependent cytotoxicity of GO beyond 75 µg/mL concentration is in agreement with the previously published results.[23] However, to the best of our knowledge, there is no study that reported the biocompatibility of bwGO with human cell lines. Chemically reduced GO was found to be much more toxic, in comparison to GO or bwGO.[40] There has been no detectable toxicity for OD, even at very high doses (500 µg/mL), which indicates that any toxic effect of GO is intrinsic to it and not necessarily due to the presence of OD in GO, but further studies may be needed to validate this interesting observation.

Conclusions

The oxidative debris, a byproduct of graphene oxide synthesis by oxidation[41] affects various mechanical, chemical, biological and optical properties of GO at various levels. This debris can be separated from GO by base wash and the resulting sheets are called base washed GO (bwGO). Our current study focused on the role of OD in governing the behavior of proteins at GO surfaces. Analysis with 13 different proteins of variable molecular and biological properties revealed that the interactions are more specific to the protein used. Arginine and aliphatic residues of the proteins controlled the mode and strength of interactions with GO and bwGO surfaces, indicating the role of hydrogen bonding, electrostatic and hydrophobic interactions. These interactions played a major role in determining the protein secondary structure and the enzymatic activities, which are crucial for GO based biodevices. The present study makes some progress in the fundamental understanding of protein behaviour at graphitic surfaces and the importance of OD in interpreting protein-GO interactions.

Acknowledgements

CVK thanks NSF EAGER grant DMR/BMAT-1441879 and AB thanks NIH ES021762 grant for the financial support of this work.

Notes and references

[1] C. Chung, Y.K. Kim, D. Shin, S.R. Ryoo, B. H. Hong and D.H. Min, *Acc. Chem. Res.*, 2013, **46**, 2211-2224.
[2] I. K. Deshapriya and C. V. Kumar, *Langmuir*, 2013, **29**, 14001-14016.
[3] R. Huang, R. P. Carney, K. Ikuma, F. Stellacci and B. L. T. Lau, *ACS Nano*, 2014, **8**, 5402-5412.
[4] Y. Zhang, C. Wu, S. Guo and J. Zhang, *Nanotechnol. Rev.*, 2013, vol. 2, p. 27.
[5] Y. Zhang, J. Zhang, X. Huang, X. Zhou, H. Wu and S. Guo, *Small*, 2012, **8**, 154-159.
[6] J. Zhang, F. Zhang, H. Yang, X. Huang, H. Liu, J. Zhang and S. Guo, *Langmuir*, 2010, **26**, 6083-6085.
[7] S. S. Chou, M. De, J. Luo, V. M. Rotello, J. Huang and V. P. Dravid, *J. Am. Chem. Soc.*, 2012, **134**, 16725-16733.
[8] I. Pavlidis, T. Vorhaben, D. Gournis, G. Papadopoulos, U. Bornscheuer and H. Stamatis, *J. Nanopart. Res.*, 2012, **14**, 1-10.
[9] Q. Mu, G. Su, L. Li, B. O. Gilbertson, L. H. Yu, Q. Zhang, Y. P. Sun and B. Yan, *J. Appl. Mater. Interfaces*, 2012, **4**, 2259-2266.
[10] A. Pattammattel, M. Puglia, S. Chakraborty, I. K. Deshapriya, P. K. Dutta and C. V. Kumar, *Langmuir*, 2013, **29**, 15643-15654.
[11] L. Jin, K. Yang, K. Yao, S. Zhang, H. Tao, S. T. Lee, Z. Liu and R. Peng, *ACS Nano*, 2012, **6**, 4864-4875.
[12] J. P. Rourke, P. A. Pandey, J. J. Moore, M. Bates, I. A. Kinloch, R. J. Young and N. R. Wilson, *Angew. Chem. Int. Ed.*, 2011, **50**, 3173-3177.
[13] R. E. M. Diederix, M. Ubbink and G. W. Canters, *ChemBioChem*, 2002, **3**, 110-112.
[14] A. Bonanni, A. Ambrosi, C. K. Chua and M. Pumera, *ACS Nano*, 2014, **8**, 4197-4204.
[15] V. R. Coluci, D. S. T. Martinez, J. G. Honório, A. F. de Faria, D. A. Morales, M. S. Skaf, O. L. Alves and G. A. Umbuzeiro, *J. Phys. Chem. C*, 2014, **118**, 2187-2193.
[16] H. R. Thomas, C. Valles, R. J. Young, I. A. Kinloch, N. R. Wilson and J. P. Rourke, *J. Mater. Chem. C*, 2013, **1**, 338-342.
[17] K. Yang, L. Feng, X. Shi and Z. Liu, *Chem. Soc. Rev.*, 2013, **42**, 530-547.
[18] W. S. Hummers and R. E. Offeman, *J. Am. Chem. Soc.*, 1958, **80**, 1339-1339.
[19] P. Du, J. Zhao, H. Mashayekhi, B. Xing *J. Phys. Chem. C,* 2014, **118**, 22249-22257.
[20] J.Pütter, Peroxidases. In *Methods of Enzymatic Analysis (Second Edition)*; Hans, U. B., Ed.; Academic Press, 1974; pp 685-690.
[21] R.F. Beers Sizer, I. W. *J. Bio. Chem.* 1952, **195**, 133-140.

[22] Q.H. Gibson, B. E. P. Swoboda, V. Massey, *J. Biol. Chem.* 1964, **239**, 3927-3934.
[23] Y. Liu, Y. Luo, J. Wu, Y. Wang, X. Yang, R. Yang, B. Wang, J. Yang, N. Zhang, *Sci. Rep.* 2013, **3**.
[24] Y. Chang, S. T. Yang, J.H. Liu, E. Dong, Y. Wang, A. Cao, Y. Liu, H. Wang, *Toxicol. Lett.* 2011, **200**, 201-210.
[25] X. Yang, X. Zhang, Z. Liu, Y. Ma, Y. Huang, Y. Chen, *J. Phys. Chem. C,* 2008, **112**, 17554-17558.
[26] C. V. Kumar, A. Chaudhari, *J. Am. Chem. Soc.* 2000, **122**, 830-837.
[27] M. M. Titirici, R. White, N. Brun, V. L. Budarin, D. S. Su, D. F. del Monte, J.H. Clark, M. J. MacLachlan, *Chem. Soc. Rev.,* 2015, **44**, 250-290.
[28] M. R. Eftink and C. A. Ghiron, *Anal. Biochem.*, 1981, **114**, 199-227.
[29] D. López-Díaz, M. Mercedes Velázquez, S. Blanco de La Torre, A. Pérez-Pisonero, R. Trujillano, J. L. G. Fierro, S. Claramunt and A. Cirera, *ChemPhysChem*, 2013, **14**, 4002-4009.
[30] Z. Ding, H. Ma and Y. Chen, *RSC Adv.,* 2014, **4**, 55290-55295.
[31] Q. Zeng, J. Cheng, L. Tang, X. Liu, Y. Liu, J. Li and J. Jiang, *Adv. Funct. Mater.*, 2010, **20**, 3366-3372.
[32] J. Kyte, R. F. Doolittle, *J. Mol. Biol.,* 1982, **157**, 105-132.
[33] P. Jain, A. Soshee, S. S. Narayanan, J. Sharma, C. Girard, E. Dujardin, C. Nizak, *J. Phys. Chem. C,* 2014, **118**, 14502-14510.
[34] A. M. Sultan, Z.E. Hughes, T. R. Walsh, *Langmuir,* 2014, **30**, 13321-13329.
[35] H. Ahn, T. Kim, H. Choi, C. Yoon, K. Um, J. Nam, K. H. Ahn and K. Lee, *Carbon*, 2014, **71**, 229-237.
[36] F. Ahmad and C. C. Bigelow*, J. Biol. Chem.,* 1982, **257**, 12935-12938.
[37] E. Wu, M. O. Coppens, S. Garde, *Langmuir,* 2015, **31**, 1683-1692.
[38] M. Calvaresi, S. Hoefinger, F. Zerbetto, *Chem. Eur. J.,* 2012**, 18**, 4308-4313.
[39] M. De, S. S. Chou and V. P. Dravid, *J. Am. Chem. Soc.*, 2011, **133**, 17524-17527.
[40] A. Bianco, *Angew. Chem. Int. Ed.*, 2013, **52**, 4986-4997.
[41][41] I. Rodriguez-Pastor, G. Ramos-Fernandez, H. Varela-Rizo, M. Terrones and I. Martin-Gullon, *Carbon*, 2015, **84**, 299-309.